JOURNAL OF PROPULSION AND POWER
Vol. 11, No. 4, July–August 1995

Dynamics of Aluminum Combustion

Kristen P. Brooks* and Merrill W. Beckstead†
Brigham Young University, Provo, Utah 84602

A study has been performed modeling both steady and unsteady combustion of aluminum. Law's steady-state aluminum combustion model has been expanded to include the effects of multiple oxidizers and their products, oxide accumulation on the surface of the burning aluminum particle, and convection. Both transport and thermodynamic properties are calculated internally for varying temperatures, relaxing the normal assumption of unity Lewis number. The aluminum combustion model has been compared to experimental data from burners, laser-ignited particles, and propellant under a variety of conditions, showing a reasonable degree of agreement. Calculations with the model show that O_2 is a stronger oxidizer than H_2O, which in turn is stronger than CO_2. The aluminum combustion model was incorporated into a computer model for predicting acoustic effects in a Rijke burner. Calculations have shown that a significant part of the increase in acoustic growth due to the addition of aluminum is due strictly to the change in the gas temperature profile. The change in temperature profile apparently causes the location of the velocity antinode to shift relative to the Rijke burner flame and thereby cause an increase in the flame response. The acoustic model agrees reasonably well with available acoustic growth rates for data where aluminum particles have been added to a propane Rijke burner.

Nomenclature

a_k = sum of the mole fractions of the oxidizers in Eq. (1)
C_p = heat capacity, J/kg
D = diffusivity, m²/s
d = particle diameter, m
F = ratio of total mass flux to mass flux aluminum
H = total flux of energy in aluminum combustion model, W/m²; heat of reaction, J/mol
j = mass flux due to diffusion, kg/m²/s
k = arbitrary constant in Eq. (1)
M = nondimensional mass flux used in Law's aluminum combustion model
m = mass flux, kg/m²/s
Nu = Nusselt number
p = pressure, N/m²
Q_r = heat production due to a reaction, W/m³; heat caused by radiation, W/m²
Q_2 = enthalpy in the region from the flame to infinity
q = heat flux, W/m²
Re = Reynolds number
r = radial distance, m; reaction rate, kg/m³/s
T = temperature, K
t = time, s
v = velocity, m/s; volume, m³
w = transport property weighting factor
x = mole fraction
η = fraction of vaporized oxide that moves toward the particle surface
θ = fraction of metal oxide that vaporizes at the flame
λ = fraction of metal that reacts with the particular oxidizing species
ν = stoichiometric mass ratio of oxide or oxidizer to metal
ξ = fraction of condensed products with move inward or outward
ρ = density, kg/m³
τ = characteristic time lag, s
ϕ = any given transport property
Ψ = arbitrary complex constant
ω_0 = angular frequency, s⁻¹

Subscripts
A = region between particle surface and flame
B = region between flame and infinity
b = burnt value
c = condensed oxide
f = flame
g = gas
i = gas species
inf = location of edge of boundary layer
p = particle
s = particle surface
v = vaporized oxide

Superscripts
$\hat{}$ = acoustic property with time dependency removed
$\bar{}$ = nondimensional mean property

Introduction

RESEARCHERS at Brigham Young University have utilized a propane-fueled Rijke Burner[1–6] to study the interaction between aluminum combustion and unstable combustion. Propane gas was chosen because of its convenience and the high flame temperature needed to ignite aluminum particles. Organ-pipe-type acoustic standing waves develop within the tube due to the interaction of the flame and the acoustics. Metal particles can be entrained in the gases and will ignite after passing through the flame. Braithewaite[1] found that addition of burning particles of aluminum and zirconium carbide increased acoustic growth. Barron[5] continued with the work of Braithewaite using the improved experimental apparatus modified by Finlinson.[3] He found that some Al and ZrC particles cause an increase in acoustic growth. However, he found that small Al particles could cause a decrease in acoustic growth at high concentrations. These observations will be considered in this article.

A mathematical model of the Rijke burner has also been developed by Raun,[4,6,7] which calculates the frequencies and acoustic growth rates in the Rijke burner both with and without particles. Raun's Rijke model also compared to Braithewaite's experimental results using a simplified model of aluminum combustion based on liquid hydrocarbon droplet

Received Aug. 17, 1994; revision received Dec. 28, 1994; accepted for publication Jan. 5, 1995.

*Graduate Student; currently at Battelle, Richland, WA.
†Professor, Chemical Engineering Department. Associate Fellow AIAA.

combustion. The model predicted an increase in acoustic growth due to the particles; however, the predicted increase was much smaller than that observed experimentally. The current efforts have been directed at resolving this discrepancy.

Background of Aluminum Combustion

Typical composite propellant combustion products include H_2O, CO, CO_2, HCl, and N_2. There is little molecular oxygen in the products. Thus, in solid propellant combustion the primary oxidizing compounds for aluminum combustion are apparently H_2O and CO_2. The aluminum reacts to form liquid Al_2O_3 with traces of gaseous aluminum hydroxides, chlorides, and substoichiometric aluminum oxides.

Aluminum Ignition

Aluminum ignition can follow two potential pathways: 1) the destruction of the protective oxide coat to allow the aluminum to be exposed to the oxidizing atmosphere or 2) the self-heating of the particle due to oxidizer diffusion through the oxide coat. The relative importance of these two pathways remains disputed. Research seems to indicate that the destruction of the metal oxide coating, rather than the self-heating, is the dominant mechanism. Generally, for the size of aluminum particles studied in the Rijke burner (e.g., 10–60 μm), the ignition temperature is believed to be in the range of 1700–2200 K.[8,9]

Basic Understanding of Aluminum Combustion

The combustion of aluminum has been found to be similar to liquid fuel droplet combustion. The reaction is believed to be limited by the diffusion of oxidizer towards the particle and the vaporized metal away from the particle surface. A flame zone develops at a distance of 1.5–4 radii from the particle surface where the oxidizer and vaporized metal meet and burn. The heat from the flame is conducted back to the surface to cause additional aluminum vaporization. However, unlike liquid hydrocarbon fuels, aluminum combustion produces a condensed phase. This condensed phase oxide forms submicron particle smoke that surrounds the particle and forms a flame trail.[10] Some of the aluminum oxide from the reaction products can diffuse back to the particle surface and have been seen as bright islets.[11] The condensation of products on the surface of the particle contributes to the growth of an oxide cap and provides additional energy that can increase the combustion rate of the particle.[12] However, the oxide cap can reduce the surface area available for combustion and radiate heat away from the particle. Both of these effects would slow the reaction increasingly as burning of the droplet progresses.

A complete understanding of aluminum combustion has been difficult to obtain for three reasons:

1) Combustion occurs around micron-sized particles, burning within milliseconds, and under very harsh temperatures.

2) The combustion characteristics vary widely over experimental conditions.

3) The experimental data have not been reproduced using similar experimental techniques and conditions to assure validity of individual data sets.

Most data have been correlated assuming the burning time to be proportional to the diameter of the original particle squared. In a limited number of cases, this law has been applied successfully; however, in general, burning time is proportional to the diameter raised to a power between 1.5–2.0. This variation may be due to experimental error, but several other explanations for the drop in exponent have been proposed. Pokhil[13] suggests that as pressure increases, the exponent drops. King[14] has shown that finite kinetics could cause a drop in exponent. Law[12] suggests that the aluminum oxide covering reduces combustion rates of large particles. Kuo[15] suggests convective effects as a primary cause for a reduced exponent. Further studies are needed to resolve this question.

Russian authors[13] have proposed a simple empirical burning rate law that allows for variations in oxidizer concentration:

$$t_r = k(d^{1.5}/a_k^{0.9}) \tag{1}$$

t_r is the reaction time, d is the diameter, and a_k is the sum of the mole fraction of the oxidizers including O_2, H_2O, and CO_2. However, Micheli and Schmidt[16] have suggested that weighting all oxidizers equally is incorrect and propose that experimental evidence contradicts such practice. This idea will be addressed later in this article.

Table 1 Aluminum combustion model comparison

Model	Analytical solution	Diffusion through condensate	Flame temperature = f(oxide condensation)	Product condensation on surface	Condensed buildup on surface	Extended condensation zone	Kinetics of Al + CO_2	Variable transport properties	Multiple oxidizers	Flame temperature = f(oxidizers)	Radiation effects	Convective effects
Brzustowski[17,18]	●	●	●								●	
Law[12]	●		●	●								
Law[19]	●		●	●		●						
King[14]							●					
Micheli[16]		●	●					●	●	●		
Kudryavtsev[22]	●	●				●						●
Gremyachkin[20]	●											●
Turns and Wong[23]	●		●	●	●					●		
Bhatia and Sirignano[24]	●		●	●						●		
Brooks[25]	●		●	●	●			●	●	●	●	●

Theoretical Models

Several models have been proposed to describe aluminum combustion. Brzustowski and Glassman[17] proposed one of the earliest models using many of the same features as hydrocarbon droplet models.[18] However, unlike droplet combustion, the aluminum flame temperature was assumed to be limited by the boiling point of the oxide, and the outward-flowing condensed oxide could inhibit the diffusion of the oxygen to the flame zone. Most later models were outgrowths of these original concepts. The salient assumptions involved in several of these models are outlined in Table 1.

Law[12] followed the basic concepts of Brzustowski and Glassman, but also included product diffusion to the particle surface and allowed for a wide range of experimental conditions. He did not elaborate on the products that would diffuse to the surface, but based on the Brzustowski and Glassman spectral observations of AlO, Al_2O, and Al near the burning surface, one assumes that the products in Law's model include the aluminum suboxides, AlO, Al_2O, etc. Law later included an extended condensation zone,[19] which was found to be important for low-temperature surroundings only. King[14] relaxed the assumption that the kinetics of the reaction were infinite. However, the uncertainty of the kinetic data used leaves the quantitative nature of his model in question. The exponent in the d^n burning law was predicted to be in the range of 1.35–1.90 for finite kinetics as compared to the value of 2.0 associated with infinite kinetics.

Micheli and Schmidt[16] included the variation of properties in the zones surrounding the flame and effects of multiple oxidizing species including CO_2, H_2O, O_2, and Cl^-. Their model includes the thermodynamic equilibrium of the reaction products and the corresponding heats of reaction. Rather than a closed-form solution as in previous models, the diffusion and energy balances were integrated numerically in a stepwise manner allowing for varying properties and compositions.

Models emphasizing convective effects have also been published in the Russian literature.[20–22] More recently, three models[23–25] have been developed based on Law's work. The Turns and Wong model follows Law's work very closely. The Brooks model extends the Law model and will be discussed later in this article. The Bhatia–Sirignano model is analogous to Law's model, but also determines the flame and surface temperatures from thermodynamic and vapor pressure data. The Bhatia model also allows for transient heating of the particle. All three models account for the condensation of oxide at the surface, and both the Brooks model and the Turns and Wong model allow for the inhibition of surface processes due to oxide accumulation.

The various models do seem to predict qualitatively the experimentally observed trends. The aluminum particle burning rate has been found to be a strong function of oxidizer concentration and particle size, but is essentially independent of pressure, which only enters into the equations through thermodynamic and transport properties.

Aluminum Combustion Model Derivation

Law's Aluminum Combustion Model

The model by Law[12] was used as a backbone for the current work because it conformed to the following criteria. First, Law's model leads to an analytical solution rather than a numerical solution. This was desirable because the current aluminum combustion model is only a single module embedded in the Rijke acoustic model. It is accessed hundreds of times within that model, and thus the need for relative simplicity. Second, Law's model is based on physically realistic parameters, most of which are available in the literature (e.g., densities, boiling points, diffusivities, heat capacities, etc.). Third, the model appears to describe the majority of the experimentally observed behavior, including a vapor phase diffusion flame and surface formation of aluminum oxide due to diffusion of suboxides from the flame.

Law's model is a diffusion-limited vapor phase combustion model based on the conservation equations of energy and species

$$\frac{\partial}{\partial t}\rho H = -(\nabla\cdot\rho v H) - (\nabla\cdot q) - (\tau:\nabla v) + \frac{Dp}{Dt} + Q_r \quad (2)$$

$$\frac{\partial}{\partial t}\rho_i = -[\nabla\cdot(\rho_i v + j_i)] + r_i \quad (3)$$

The model assumes that as the aluminum particle burns, a fraction of the products remains as vapor and a fraction condenses. This oxide vapor that is created at the flame can diffuse both towards the particle surface and towards the surroundings. The oxide vapor that diffuses to the particle surface condenses, resulting in increased aluminum vaporization. The vapor that diffuses to the surroundings may or may not condense. The condensed phase is convected away from the flame zone based on the bulk gas motion. The vapor that diffuses to the surroundings and the condensed phase do not appear to impact the particle combustion rate significantly.

The mass fluxes of the various species between the particle and the flame (region A) and between the flame and infinity (region B) are based on the mass flux of metal M_f away from the surface of the particle (see Table 2).

The symbols θ and η represent the fraction of oxide product that is vaporized and the fraction of vaporized product that moves toward the particle surface, respectively. The symbol ν is the stoichiometric mass ratio of oxide product p or oxidizer i to metal. The symbol λ is the fraction of metal that reacts with a particular oxidizing species. ξ_A and ξ_B are the fraction of condensed products that move inward or outward, respectively. The total flow in these regions is determined by separately summing the terms involved with inward flow and outward flow. Assumptions of the model include pseudo-steady-state burning, spherical symmetry, negligible viscous forces, isobaric conditions, infinitely thin flame zone, negligible volume fraction of the oxide smoke, burning aluminum particles at their boiling points, and Fick's and Fourier's laws.

After integration and application of the boundary conditions at the flame, the equations of energy and species take on the form

$$\dot{m}(r^{-1} - r_f^{-1}) = -4\pi\rho_g D_i \times \nu\left[1 - \frac{\dot{m}C_p(T_f - T)}{\dot{m}C_p(T_f - T_s) - \dot{m}_v Q - \dot{m}_v Q_1 - H}\right] \quad (4)$$

$$\dot{m}(r^{-1} - r_f^{-1}) = 4\pi\rho_g D_i \nu\left(\frac{\dot{m}Y_{i,f} - \dot{m}_i}{\dot{m}Y_i - \dot{m}_i}\right) \quad (5)$$

for both the regions between the particle and the flame and between the flame and infinity. The mass fluxes of reactants and products are determined by stoichiometry and the heat flux H determined from the conditions at the particle surface. These equations can then be combined and the mass flux $\dot{m}$ removed from the solution. The ratio of condensed to vaporized oxide or the flame temperature is determined from these equations. Once a solution is obtained, the mass flux of aluminum can be calculated and the burning time determined.

Unlike other similar models, Law includes the effects of product diffusion to the surface of the particle. Law also makes an effort to account for the directions of bulk flow, as they are responsible for the motion of the condensed phase oxide product. Four potential modes of burning are postulated, based on the temperature and composition of the surrounding gas (see Fig. 1 and Table 3).

Table 2 Mathematical descriptions of species in the aluminum combustion model

Species	Region A	Region B
Vaporized metal	M_f	——
Oxidizer species i	——	$M_{i,B} = \lambda_i \nu_i M_f$
Vaporized metal oxide	$M_{v,A} = -\theta v_p \eta M_f$	$M_{v,B} = \theta v_p (1 - \eta) M_f$
Condensed metal oxide	$M_{c,A} = -(1 - \theta) v_p \xi_A M_f$	$M_{c,B} = (1 - \theta) v_p \xi_B M_f$

Table 3 Modes of aluminum combustion

Gas temperature or oxidizer concentration	Flow direction		Flame temperature	Fraction of oxide vaporized
	Between flame and particle	Between flame and infinity		
Low	Outward	Inward	$<T$ boil	0
Medium	Outward	Inward	at T boil	0–1
Medium	Outward	Outward	at T boil	0–1
High	Outward	Outward	$>T$ boil	1

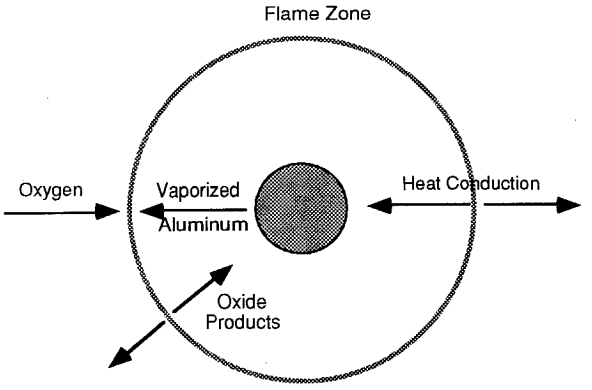

Fig. 1 Schematic diagram of Law's aluminum combustion model.

At low gas temperature or oxidizer concentration, the motion of the gas is toward the flame and the flame temperature is below the boiling point of the oxide. With increased temperature or oxidizer concentration, the flame temperature reaches the boiling point of the oxide and the fraction of vaporized oxide begins to increase. Higher quantities of vaporized oxide result in an increase in diffusion of matter away from the flame and the gas flow between the flame and infinity switches directions. At high gas temperature or oxidizer concentration, all the oxide is vaporized and the flame temperature once again rises with increased concentration or surroundings temperature.

Modifications to Law's Model

Several of the original assumptions made in Law's model have been relaxed and are tabulated in Table 4. A schematic diagram of the features included in the modified model are shown in Fig. 2.

By applying the boundary conditions at the particle surface, flame, and at infinity, a set of equations describing the species concentration and temperature in the inner and outer region results as seen in Table 5. These equations are then combined to form $i + 1$ independent equations and $i + 2$ unknowns (where i is the number of oxidizing species). To complete the degrees of freedom (DOFs), we recognize that the sum of the fraction of oxidizer must be equal to one. The $i + 2$ equations are solved using a multivariate Newton–Raphson technique. Relaxation must be included for the equations to reach convergence.

To achieve an analytical expression, the integration of the energy and species equations assumes constant properties in the regions between the particle and the flame (region A) and between the flame and infinity (region B). Averaged transport properties are determined for each of these regions, by weighting the properties at the particle surface s, flame f, and at infinity ∞, according to Chung and Law[26]:

$$\phi_{A,B} = [1/(w + 1)](\phi_{s,f} w + \phi_{f,\infty}) \tag{6}$$

where ϕ is any given transport property. A value of two is used for the weighting factor w, as suggested.[26] These property values are allowed to vary throughout the solution as the concentration of the gaseous species vary during the combustion process. In addition, the Lewis number is not constrained to unity.

Finally, the improved model allows for multiple oxidizers including water, carbon dioxide, and oxygen, since all three are present both in the Rijke burner and in propellant exhaust gases. Other models have been based on oxygen only.

Heat and Mass Transfer Effects

Convection effects were accounted for using the Frank–Kamenetski[27] "reduced-film" approximation as in Gremyachkin's model.[20–21] This approximation consists of choosing some "region of influence" around the particle in which the change in temperature and concentration occurs. Outside this layer, the temperature and concentrations are assumed to be at the bulk value. This approach works reasonably well for the steady-state modeling of aluminum; however, it should be noted that it does not describe the characteristics of fluctuating aluminum combustion.

Heat transfer by radiation is treated solely as gray-body emissivity between the flame and the particle surface and the flame and the surroundings. The oxide smoke, not the gaseous flame, is responsible for the majority of the radiation from the flame to the particle surface. Determining the optical thickness of the oxide smoke has not been addressed in this study.

Oxide Buildup on the Particle Surface

Finally, an understanding of the condensed oxide on the surface of the particle has been considered important by many experimentalists.[11,28,29] In order to account for the change in combustion rate due to surface coverage of condensed aluminum oxide, the burning rate is proportioned according to the surface area covered by the oxide to the surface area if no oxide were present. According to pictures taken of partially burned particles,[28] the aluminum and oxide "cap" can be approximated as fractions of attached spheres. For modeling purposes the smaller cap has been assumed to be a half-sphere, while the larger aluminum particle is assumed to be

Table 4 Comparison of original law model and modified model

Law model assumptions	Assumptions of the modified model
Properties constant everywhere	Calculation of properties based on weighted average of properties at particle surface, flame, and infinity
Oxygen only reactant	Multiple species allowed with variable transport and thermodynamic properties
Burning in stagnant gas	Convective effects based on the Nusselt number
Radiation neglected	Radiation between particle, flame, and surroundings
Lewis number = 1	Allows Lewis numbers different than 1
Oxide on particle surface has no effect	Reduced burning rate due to oxide surface coverage.

Table 5 Species concentration and temperature equations in regions A and B

	Region A
Aluminum	$M_f F_A \left(1 - \frac{1}{\hat{r}_f}\right) = -\nu_{Al}[1 - F_A Y_{f,s}]$
Vaporized oxide	$M_f F_A \left(1 - \frac{1}{\hat{r}_f}\right) = -\nu_{Al}\left[1 + \frac{F_A Y_{v,f}}{\theta \nu_p \eta}\right]$
Temperature	$M_f F_A \left(1 - \frac{1}{\hat{r}_f}\right) = Le_A \nu_{Al}\left[1 + \frac{F_A(\hat{T}_f - \hat{T}_s)}{1 - \hat{Q}_2 \theta \nu_p \eta - \hat{Q}_{r,A}}\right]$
	Region B
Oxidizer	$M_f F_B \left(\frac{1}{\hat{r}_{inf}} - \frac{1}{\hat{r}_f}\right) = -\nu_{Al}\left[1 + \frac{F_B Y_{i,\infty} D_f}{\lambda_f \nu_f D_B}\right]$
Vaporized oxide	$M_f F_B \left(\frac{1}{\hat{r}_{inf}} - \frac{1}{\hat{r}_f}\right) = \nu_{Al}\left[1 - \frac{F_B Y_{v,f}}{\theta \nu_p (1 - \eta)}\right]$
Temperature	$M_f F_B \left(\frac{1}{\hat{r}_{inf}} - \frac{1}{\hat{r}_f}\right) = -Le_B \nu_{Al}\left[1 - \frac{F_B(\hat{T}_f - \hat{T}_\infty)}{F_B(\hat{T}_f - \hat{T}_s) - \phi_2}\right]$

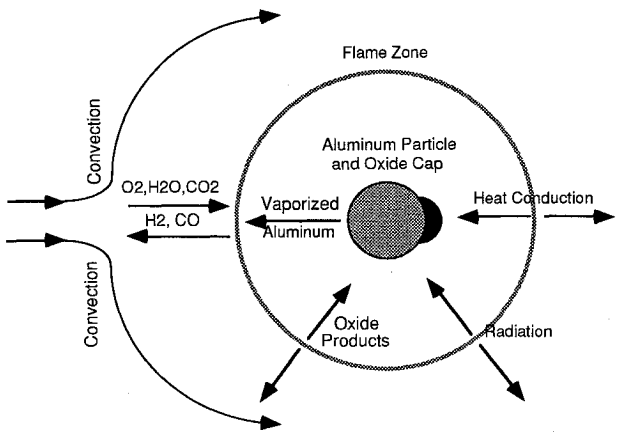

Fig. 2 Schematic diagram of aluminum combustion model used in this study.

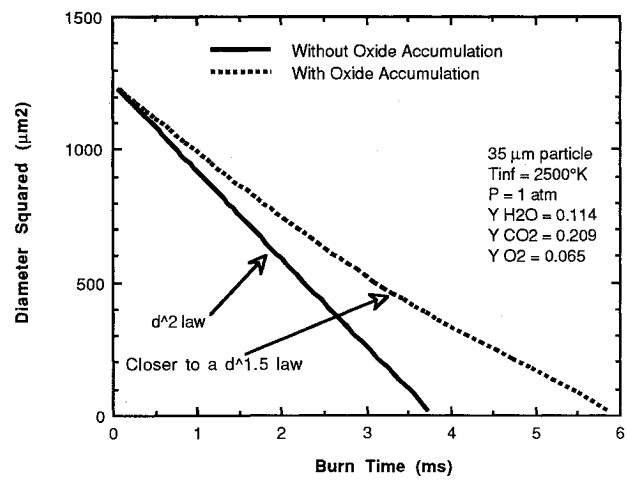

Fig. 3 Effect of oxide accumulation on the particle surface.

a partial sphere, restricted by the cap. During the combustion process the cap grows due to the diffusion of the oxide vapors to the surface, while the aluminum particle decreases in size due to its combustion rate. These rates are converted to volumetric changes using the densities of the materials. The volume changes are then related to the change in surface area available for combustion. As the aluminum particle burns out, a residual oxide cap remains. This concept is normally equated to combustion of agglomerates, but the model also indicates that it is important with any particle of aluminum. Results are presented in the following section.

Results of the Steady-State Aluminum Model

To evaluate the model, a parametric study was performed and the results compared to experimental results available in the literature. A description of the results of these parametric studies follows.

Effect of Particle Diameter

Figure 3 shows the calculated particle diameter as a function of time. Initially, the oxide cap on the particle is not sufficiently large to inhibit burning significantly, as the particle burns over virtually the entire surface. However, as oxide accumulates, the burning rate slows due to the decreased surface area. The predicted instantaneous burning rate appears to be correlated by a $d^{1.5}$ law, due to the variation in surface area caused by the oxide accumulation. However, when comparing the overall burning times for different particles, the general D^2 law seems to hold.

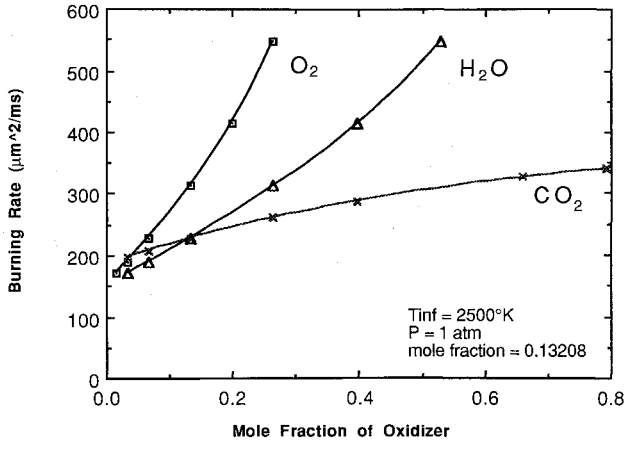

Fig. 4 Calculated aluminum burning rates showing the effect of oxidizer concentration, holding the other two species constant.

Effect of Concentration

It has been suggested by numerous experimentalists that the burning time is inversely proportional to the oxidizer concentration.[30] The Russian empirical correlation [Eq. (1)] suggests that the burning rate is proportional to the total oxidizer mole fraction to the 0.9 power. In both cases, the oxidizer concentration is summed. This implies that all oxidizers have similar effects on the burning rate. Using the model to test these assumptions, it was found that each oxidizer has a different effect on the burning time and their values cannot simply be summed together (see Fig. 4). Oxygen has the greatest effect on the burning rate and CO_2 has the smallest effect.

A more appropriate correlation appears to be

$$t_b = C\left(d^2 \Big/ \sum c_i x_i\right) \tag{7}$$

where C is a constant based on ambient temperature and pressure, and c_i and x_i are the constants and mole fractions for the individual oxidizing species, respectively. The concentration was varied over a range of approximately 200% for each species. For conditions similar to those found in the Rijke burner, the values of c_i for O_2, H_2O, and CO_2 were calculated from Fig. 4 to be 1.0, 0.533, and 0.135, respectively.

These results are not surprising considering the higher heat of reaction associated with oxygen. Also, oxygen has twice as much oxidizer per mole as the carbon dioxide, which should enhance the combustion rate of oxygen relative to carbon dioxide. If the constants are normalized with respect to the heat of reaction on a per weight basis multiplied by the diffusivity, the oxidizer effects become nearly equal. This result stems primarily from oxygen having a higher heat of reaction. Water and carbon dioxide have comparable heats of reaction, but water has a lower molecular weight and a higher diffusivity. Carbon dioxide has only a marginal effect as an oxidizer. These results suggest that the simple summing of oxidizers is inadequate and cannot account for the differences in heats of reaction, stoichiometry, transport properties, and products formed from oxidizer to oxidizer.

Changes in the flame standoff distance with respect to oxidizer concentration were also investigated. It was found that for conditions similar to those in the Rijke burner, the dimensionless flame radius increases with the addition of oxygen from a value of 1.5–2.5. With an increase in water concentration, the same dimensionless flame radius decreases from 2.5 to 2.0. With an increase in carbon dioxide concentration, the flame radius remained almost constant at a value of ~2.2. These results are qualitatively similar to numerous experimental investigators,[13,31] who report a dimensionless flame radius of ~1.5 for atmospheres with water and ~3 for oxygen.

Effect of the Surroundings

An increase in ambient gas temperature resulted in an essentially linear increase in burning rate when the flame temperature is lower than the boiling point of oxide. As the flame temperature reaches the oxide boiling temperature (at an ambient temperature of approximately 1500 K), the slope of the curve increases.

The effect of the particle being immersed in a flowfield was also investigated. Under stagnant conditions, the Nusselt number of a sphere has a value of 2. In the model, the burning time is not effected by convection between Nusselt number values of 2 and 2.1. For Nusselt numbers larger than 2.1, both the burning time and the flame radius decrease.

Kuo[15] has suggested that in high flow conditions, the burning rate is changed from a d^2 law to a $d^{1.5}$ law due to convective effects. This result stems from the fact that for a sphere, the Nusselt number can be represented as $Nu = 2 + cRe^{0.5}$. As the Reynolds number gets very large, the Reynolds number dominates the value of the Nusselt number. The $d^{0.5}$ in the Reynolds number then causes the exponent in the burning time to drop to 1.5. As the Reynolds number approaches infinity, the equations in this model also give the same result. However, using Reynolds numbers up to 25, the burning time correlation in the model was found only to drop to $d^{1.88}$ due to high convective flow. It was not possible to simulate higher flows due to numerical convergence difficulties. Additionally, Reynolds numbers greater than 25 are probably not realistic.

Additional Parameters Investigated

The relative effect of several parameters in the model that are not well-quantified, but that were studied parametrically are discussed below.

Radiation

For particles less than 40 μm, radiation between aluminum particles and condensed oxide at the flame has little effect for emissivities between zero and one. For particles 50–100 μm and a flame emissivity of one, heat radiated from the flame to the particle has a larger effect (e.g., a 10–20% decrease in burning time). Realistically, the emissivity of the flame only becomes large when oxide has accumulated in the flame zone. This will occur when the particle is near burnout and is small. Thus, radiation to the aluminum droplet should actually have little effect on the overall burning time of an individual particle.

Transport Property Weighting Factor [Eq. (6)]

By weighting the properties either totally by the conditions at the flame or totally by the conditions at the particle surface and infinity, a maximum change of 50% in burning rate results.

Heat of Vaporization

Although aluminum vaporization during combustion is usually considered to be due only to the boiling of aluminum liquid at the particle surface, it has been postulated that surface oxides react with the molten aluminum to form suboxides that also leave the particle surface. Thus, the value of the heat of vaporization may not be a simple boiling phenomenon,[21] but could well be a reactive dissociation such as

$$Al_2O_3(l) + Al(l) \rightarrow Al(g) + Al_2O(g) + AlO(g) \tag{8}$$

To evaluate this possibility within the model, an arbitrary 50% increase in the heat of vaporization yielded a 25% decrease in the particle burning time. This is an idea that needs more study.

Diffusion to Surface

An increase in the diffusion of oxide to the surface was shown to increase the reaction rate by as much as 45% in the

model. This result is due to the increased heat release from vaporized aluminum suboxides condensing on the surface of the particle. In this scenario, it was assumed that all the energy from oxide condensation goes into the particle to vaporize additional aluminum. It was further assumed that oxide condensing on the surface reacts with aluminum and leaves the surface rather than forming an oxide cap. Even with these restrictive assumptions the effect of diffusion to the surface is significant.

Oxide Accumulation on Surface

The oxide accumulation on the particle surface covers part of the area where aluminum would vaporize from the surface and slows the reaction rate. Considering this effect without including the additional heat that would be generated from condensation of oxide (as in 4), the model shows a slowing of the reaction rate by approximately 25% due to surface coverage. Again, this is a phenomenon that needs further study.

Overall, it appears that the diffusion and condensation of oxide on the surface is a larger effect than oxide accumulation on the particle surface. Further studies are needed to quantify which suboxides diffuse to the surface and how they react there. Also, more quantitative information is needed on heterogeneous reactions between the aluminum and various oxides, both at the surface and within the particle. For tractability these reactions have been neglected.

Comparison with Experimental Results

Experimental results from several sources were compared to the model to determine its accuracy and versatility. Experimental data were found that came from aluminum ignited in gas burners, laser drop tube experiments, and propellant experiments. Calculations were made for each data set considering the two extremes:

1) Oxide diffuses back to the surface and its condensation provides energy to the particle, resulting in increased reaction rate.

2) Oxide on the surface forms a cap, reducing the effective reaction area, thus slowing burning. The data are compared to the calculations in Fig. 5, plotting the surface burning rate determined by the two approaches.

Experimental results from gas burners were taken from Friedman and Macek.[8,32,33] The upper error bar values represent the calculation that allows diffusion of oxide back to the surface of the particle and no oxide cap forms. The lower error bar values represent the calculation with no diffusion of oxide back to the surface of the particle. The model generally compares very well to these gas burner experimental results. Most of the disagreement is believed in these cases to be associated with small particles burning very rapidly (e.g., $\leq$4 ms). Error probably stems from experimental difficulties in measuring such short burning times.

Aluminum combustion data for laser-ignited particles were reported by Prentice[29] and Wilson and Williams.[31] The data were taken at lower temperatures and generally higher oxygen concentrations. Primary oxidizers were oxygen and carbon dioxide with traces of water vapor present. Only data taken at oxygen concentrations lower than 30% were considered because fragmentation occurs at higher oxygen concentrations, confusing the data. The upper portion of the error bar seems to fit the data best. This result suggests that oxide diffuses to the particle surface, increases the reaction rate, but does not form a nonpenetrable oxide cap.

Propellant experiments performed by Davis[30] and Hartman[34] provided the third data set. Unlike the other data sets that were performed near atmospheric pressure, their work was done at typical rocket pressures (~20 and 50–68 atm). For the lower pressure data, the model follows experimental trends reasonably well. However, the higher pressure experimental results indicate a substantial increase in burning rate that the model does not predict. Pressure only enters the model in the temperature-dependent properties associated with increased particle and flame temperature. For this reason, the model only predicts a 20% increase in burning rate over the range of 14–1000 psia; much lower than apparently observed experimentally. Further work is needed to determine the pressure effect, either from an experimental or modeling perspective.

The model has also been compared to the more recent data of Turns and Wong[23,35] in Fig. 6. The model calculates burning times of ~25–30% longer than the experimental times. Also, the calculated dependence on diameter gives an exponent of ~2, while the data give an exponent of ~1.8. The source of these discrepancies could not be ascertained within the model nor within potential sources of experimental error.

It is informative to compare these calculations with those made by other models. Calculations with the Turns–Wong model[23] bracket the data depending on their assumption relative to the surface inhibition due to the oxide cap. If they assume that the cap inhibits the available surface area (as in the current model), their calculated times are ~40% longer than those measured. If there is no inhibition, their calculated times are just slightly less than the data. In the Bhatia–Sirignano model[24] their calculated times are in excellent agreement with the 10% O_2 data of Turns and Wong. The calculated diameter exponent for both the Bhatia–Sirignano model and the current model is ~2, whereas the Turns–Wong data indicate a value of 1.77 $\pm$ 0.20. A final area of comparison is the calculated dependence on oxygen concentration. Tests in 25% O_2 show a reduction in burning times of ~45% over tests with 10% O_2. Calculations from the Turns–Wong model and the current model both reproduce the ~45% reduction in burning times. However, the Bhatia–Sirignano overpredicts the O_2 concentration dependency, calculating a reduction in burning times of ~65% for the two cases.

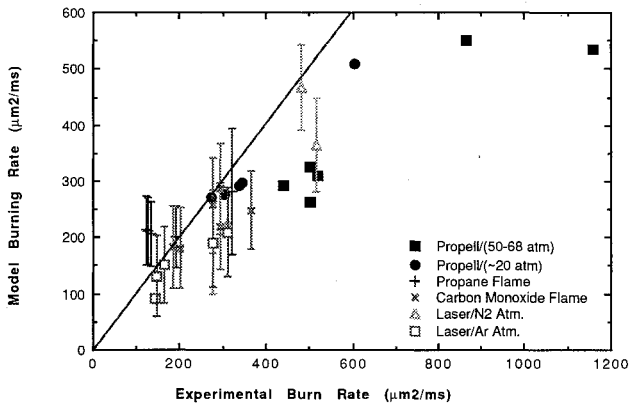

Fig. 5 Comparison of model to experimental data.

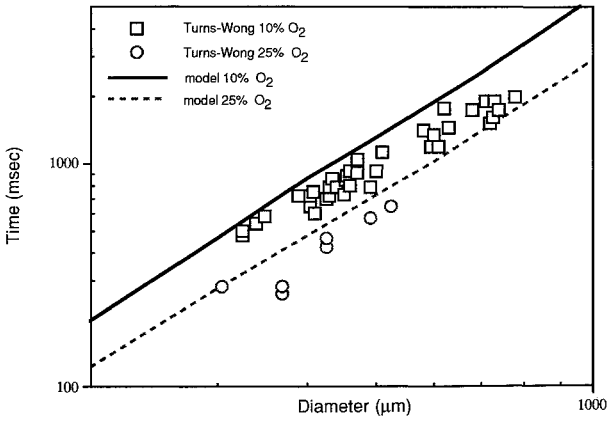

Fig. 6 Comparison of model to experimental data of Turns and Wong.

Each of the three models compared here are either a direct derivative of, or are very similar to, Law's model.[12] Thus, it is not surprising that they produce very similar results. However, there are also significant differences. The Bhatia–Sirignano model seems to have the best agreement with the basic data (i.e., the 10% O_2 data). The Turns–Wong model is closer to agreement with the data if the surface inhibition due to the oxide cap is neglected. In the current model this is also true. Thus, the method of calculating the oxide cap inhibition of the reacting surface area apparently is not simulating the real physical phenomenon accurately. Also, it is not clear why the Turns–Wong model seems to predict the diameter dependence better than the other two models, nor is it clear why the Bhatia–Sirignano model overpredicts the dependency on O_2, while the other two models seem to predict it correctly. Further studies are needed to clarify the physical characteristics that result in these apparent discrepancies.

Each of the three models also calculate the size of the oxide cap formed from the combustion. Both the Turns–Wong and the Bhatia–Sirignano models calculate oxide caps of ~65% of the original aluminum agglomerate. This is in good agreement with the data reported by Turns and Wong. In the current model oxide cap diameters of ~90% were calculated, but these correspond to the density of the oxide at the temperature of the oxide used within the model (i.e., the boiling point of the oxide, ~4000 K). If the size of the oxide cap is recalculated using the density corresponding to ambient conditions, the size of observed caps would be ~60–65% of the original aluminum. Thus, all three models are in agreement with this observation.

Interactions of Acoustics and Aluminum Combustion

In the Raun Rijke acoustic model[6,7] mean properties do not vary with time and are solely a function of location in the burner. Oscillatory properties describe the acoustics and are a function of location in the burner and frequency. Solution of the equations describing the oscillatory properties in the burner require a knowledge of the variations in mean properties of the gas and the particles in the hot section. To obtain profiles of these mean properties, the location and rate of aluminum combustion must also be known.

Ignition Delay

Knowing the location of particle ignition is important to allow for the proper calculation of mean properties. In the current work, the terms responsible for particle convection of momentum and energy

$$\rho_p v_p \frac{\partial v_p}{\partial x} \quad \text{and} \quad \rho_p v_p \frac{\partial h_p}{\partial x} \tag{9}$$

have been incorporated into the continuity equations to allow for the influence of acceleration and heat-up on ignition delay. Ignition is assumed to occur when the particles reach some specified temperature.

To determine a reasonable ignition temperature, the unsteady energy equation including convective terms was solved. This simple stand-alone model was compared to available experimental results. With a melting point of aluminum oxide of ~2300 K, and considering thermal stresses during heat-up, ignition temperatures in the range of 1600–2300 K were considered. The assumed ignition temperature was adjusted until ignition delay times matched the experimental work of Friedman and Macek[8] and Davis,[30] with the best fit occurring for an ignition temperature of approximately 1900 K. Using values of 1600 resulted in calculated ignition delay times approximately 30% low, while values of 2300 resulted in values ~30% high. Thus, the value of 1900 was used in all other calculations in the Rijke acoustic model to determine the location of aluminum ignition in the burner.

The ignition delay times calculated by the expanded Rijke acoustic program were then compared to the solution of the simple stand-alone computer model. Equations describing both the energy and momentum of a single particle were solved in order to determine if the step size of the Runge–Kutta calculation was sufficiently small to properly calculate ignition delay. The results of the Rijke program were found to differ by less than 5% from the results of the simple model for particles in the range of 15–65 μm in diameter.

Aluminum Combustion Model

The features of the modified aluminum combustion model were incorporated into the Rijke acoustic model, and the results compared to the stand-alone aluminum model. Differences of less than 5% were determined, which was deemed acceptable.

Within the model heat transfer can occur between gas and particle phases in the following ways: 1) convective heat transfer between the particles and the gas, 2) radiation between the particles and the surroundings, 3) production of heat due to the reaction of aluminum with its oxidizer, and 4) heat loss from the gases to the surroundings. Calculated gas temperature profiles are shown in Fig. 7 varying the oxide emissivity and the percentage of aluminum. In most respects the curves follow expected trends. However, for values of oxide emissivity greater than 10%, the outlet gas temperature with aluminum addition is actually lower than the case with gas only. It appears that heat from the gas is convected to the oxide particles and then radiated to the surroundings, reducing the exhaust temperature.

Acoustic Properties in the Rijke Burner

Raun used a linear perturbation of a liquid droplet combustion model to describe the fluctuating particle reaction rate. His acoustic growth rates due to the fluctuating aluminum combustion for an acoustically inactive burner flame were an order of magnitude lower than those observed experimentally by Braithewaite. These results provide motivation for the current modeling work.

The fluctuating aluminum reaction rate is calculated using a linear perturbation equation:

$$\hat{r}_p = \frac{\partial r_p}{\partial T_g}\hat{T}_g + \frac{\partial r_p}{\partial p}\hat{p} + \frac{\partial r_p}{\partial \rho_p}\hat{\rho}_p + \frac{\partial r_p}{\partial v_g}\hat{v}_g \tag{10}$$

where the derivatives of the particle reaction rate r_p are calculated numerically from the modified aluminum combustion model. Once again the acoustic growth rates calculated with the improved model were an order of magnitude lower than those seen experimentally. Subsequently, three reasons for the discrepancy were examined: 1) an incorrect form of the particle reaction rate equations, 2) incorrect interactions be-

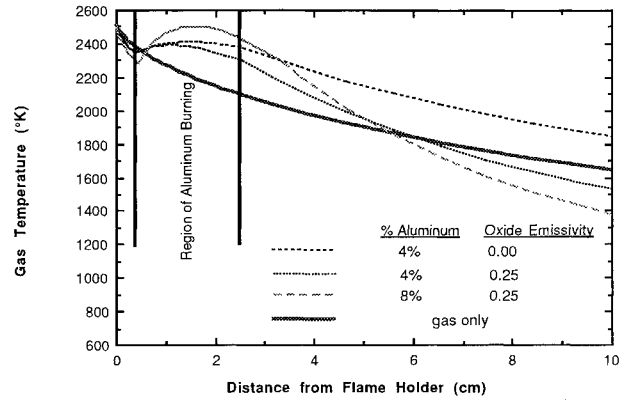

Fig. 7 Gas temperature for 25-μm aluminum particle for various emissivities and percentages of aluminum.

tween the particle reaction model and other parts of the Rijke model calculation, and 3) limiting assumptions of perturbation theory.

Form of Particle Reaction Rate

Both Raun's Rijke model and the one of this study assume the aluminum reaction rate is diffusion limited. To test the possibility that the reaction rate could be kinetic limited instead, the particle reaction rate was assumed to be an Arrhenius function of the surface temperature. For reasonable values of the order of the reaction ($n = 2$) and the activation energy ($E_a = 40{,}000$ cal/mole), the values of the perturbed reaction rate continued to be an order of magnitude too small, suggesting that the form of the equation is not the primary reason for the discrepancy between the model and experiment.

To determine what form the reaction rate expression should take and the magnitude of the parameters required to produce the proper results, an empirical fluctuating reaction rate equation of the form

$$\hat{r}_p = (\Psi_p \hat{p} + \Psi_v \hat{v}_g)\bar{r}_p \tag{11}$$

(where Ψ is an arbitrary complex constant) was assumed. Calculated acoustic growths of the proper magnitude could only be achieved for values of Ψ_p, the pressure-dependent complex constant, real and on the order of 10^{-3}, and values of the velocity-dependent complex constant, Ψ_v, imaginary and on the order of 1. These results suggest that the fluctuating reaction rate must be in phase with the pressure and 90 deg out of phase with the acoustic velocity, similar to what would be expected by the Rayleigh criteria.[36]

Interactions between Particles and Flame

To evaluate the possibility of acoustic interactions between the particle reaction rate and the propane flame, the revised Bailey flame model (as used by Raun; see also Bailey[37]) was used to make parametric calculations of the flame response without the effects of the fluctuating aluminum reaction rate (but allowing for the mean particle combustion effects). Model results indicated that the addition of aluminum particles increased the acoustic growth (see Fig. 8), similar to that seen experimentally, in spite of the fact that the fluctuating aluminum combustion terms in these calculations were set to zero. This surprising result seems to indicate that the addition of aluminum changes the mean properties of the burner sufficiently to cause changes in the propane flame response without the need for the fluctuating heat release due to the particles.

This phenomenon can be explained as follows. The acoustic mode shape and location of nodes and antinodes of the standing wave are determined by the temperature profile within the burner. If the temperature profile is changed, then the location of the acoustic nodes and antinodes in the burner is also changed. Maximum driving occurs when the velocity antinode is located at the Rijke burner flame. Changes in the temperature profile due to aluminum combustion can move the velocity antinode towards the flame, resulting in an increase in acoustic growth, or away from the flame, resulting in a decreased acoustic growth. For all of the conditions and Rijke flame models studied, this "indirect" mechanism of distributed combustion can be a significant portion of the acoustic growth (e.g., 30–100% of the total increase due to the aluminum particle addition).

Key particle parameters effecting this indirect aspect of distributed combustion include the weight percent aluminum added to the burner and the emissivity of the smoke created. Initial aluminum particle diameter and oxidizer concentration have a somewhat lesser effect on the mode shift. Ignition temperature has very little effect on the acoustic growth change.

Oxide emissivity has the largest effect on the acoustic growth. Although the emissivity of a single particle of oxide is quite well-quantified (e.g., 47% at 1500 K), the effective emissivity of a cloud of oxide particles is more difficult to determine. Raun used a value of 0.25 for the emissivity of the oxide. Glassman[38] suggests that, in a cloud of particles, there are little radiative heat losses because a single particle sees primarily particles of the same temperature. A reasonable emissivity value for a cloud may well be very small. Calculations were made varying the emissivity from small values up to the single particle value. As exhibited in Figs. 7 and 9, an increased value of emissivity causes a significant drop in hot section temperature profile, and a significant increase in the calculated acoustic growth. Because of its importance in defining the temperature profile and the acoustic growth rate, further study is needed in this area.

As evidence of the indirect mechanism of distributed combustion, Barron[5] noted an increase in acoustic growth in the Rijke burner with the addition of aluminum oxide particles. This increase was originally attributed to some possible catalytic effect. Because aluminum oxide does not burn, the direct distributed combustion effects due to fluctuating reaction rate would not be present. It would not seem unreasonable, however, that the introduction of the aluminum oxide would cool the hot section of the burner sufficiently either due to heat absorbed or radiated to cause a shift in the acoustic mode such that the acoustic velocity antinode was nearer the flame. This would result in the increased acoustic growth seen experimentally.

In addition to changes in the acoustic growth due to a mode shift, the Rijke burner flame model increases the magnitude of the acoustic properties in the hot section of the tube. Such

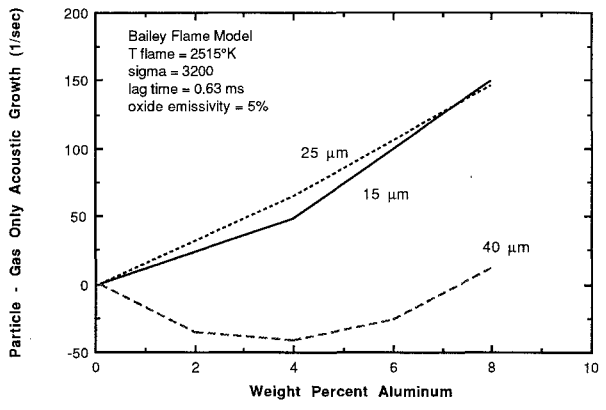

Fig. 8 Calculated acoustic growth rate vs percent aluminum for the revised Bailey flame model using various sizes of aluminum.

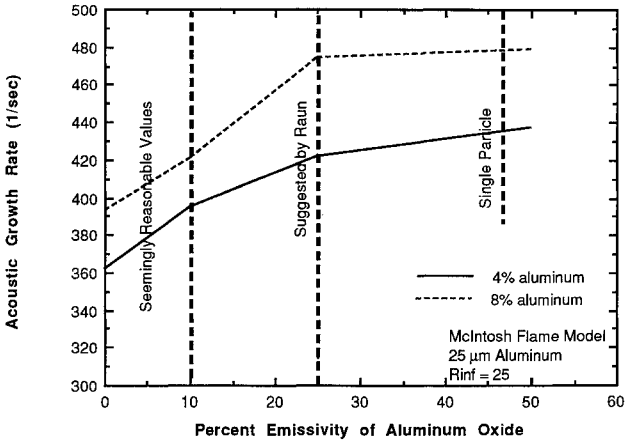

Fig. 9 Rijke acoustic model calculated acoustic growth rate as a function of aluminum oxide emissivity. Increased emissivity causes a drop in hot section temperature profile.

increases yield increased values of the fluctuating reaction rates as Eq. (11) would suggest. Therefore, the acoustic growth due to the fluctuating particle reaction and flame can couple to give a much larger value than their individual components. Parametric calculations showing this result are illustrated in Fig. 10.

Limiting Assumptions of the Perturbation Theory

A third reason for the difficulty in fitting the experimental data with the acoustic model is the limiting assumptions of the perturbation theory. Two difficulties are encountered when using simple perturbation theory to solve for the fluctuating particle reaction rate rather than solving the unsteady conservation equations in their entirety. The first difficulty is that of taking derivatives of empirical correlations. The majority of the aluminum combustion model is based on conservation equations. Taking derivatives of these equations should be possible without losing the physical nature of the solution. In contrast, calculation of the derivative of the reaction rate with respect to velocity requires the use of a Nusselt number correlation. Unlike continuity equations, the Nusselt number correlation is created by fitting experimental data. The functional form of the correlation may not be physically correct. Therefore, when the derivative is taken it may not represent physical reality. Error from perturbing such empirical correlations is difficult to determine, but may be significant.

A second difficulty associated with perturbation theory is that the reaction rate is assumed to respond instantaneously to the acoustic properties. For a diffusion-limited process, it would seem that changes in the bulk of the fluid would not have an instantaneous effect on the fluctuating reaction rate or heat release, but that there would be a lag time associated with the aluminum combustion.

Further evidence of the need for a lag time can be seen in the results of using the Bailey flame response to model the propane flame in the Rijke burner. The Bailey model is based on two parameters: 1) a flame ignition delay time and 2) the derivative of the flame speed with respect to the flameholder. Measured propane flame time lags are on the order of microseconds. With a time lag of microseconds, little to no acoustic growth resulted. To obtain the acoustic growth rates due to burning aluminum shown in Fig. 8, the flame ignition delay time in the Bailey model had to be on the order of milliseconds. A time lag of milliseconds is actually more characteristic of particle combustion, and not the premixed propane flame of a Rijke burner that the model was designed to describe. Thus, the Bailey flame model can produce results similar to experiment by simulating the time lag associated with burning particles. Although strictly an artifact of the mathematical model, such a result does suggest the need for a time lag in the aluminum combustion model.

In an effort to account for such a lag, the fluctuating reaction model was modified to include a delay time of the form

$$\hat{r}_p = \left(\frac{\partial r_p}{\partial T_g}\hat{T}_g + \frac{\partial r_p}{\partial p}\hat{p} + \frac{\partial r_p}{\partial \rho_p}\hat{\rho}_p + \frac{\partial r_p}{\partial v_g}\hat{v}_g\right) e^{-i\omega_0\tau} \quad (12)$$

where the first part of the term is from the original model [Eq. (10)] and the exponential term accounts for the time delay. In the exponent, ω_0 is the frequency of oscillation and τ is the lag time. This time lag is based on the time required for the oxidizing species and temperature effects in the bulk to be felt at the flame surrounding the aluminum particle. Its value is calculated from the steady-state aluminum combustion model. The problem becomes one of determining the thickness of the region through which changes in acoustic properties must travel to influence conditions at the aluminum diffusion flame (r_{inf}). The thickness of this region can be no greater than the interparticle distance and no less than at the flame front. Calculated values of the interparticle distance vary from ~40 diameters at 15% particles to ~80 diameters at 2%. The actual location of the boundary layer (or r_{inf}) is believed to be somewhere between the flame front and this interparticle separation distance.

Parametric calculations were made varying values of r_{inf}, which show a maximum acoustic growth for a value of 25. This compares favorably to a calculated value of 20 for a coal particle in Stokes flow.[39] Not surprisingly, this maximum corresponds to a 90-deg phase shift. With this phase shift, the energy release due to a velocity perturbation would be in phase with the pressure as predicted by the Rayleigh criterion.

As mentioned previously, the fluctuating reaction rate without the time lag was an order of magnitude too small. By including the lag, the acoustic velocity component of the reaction rate becomes dominant over the acoustic pressure component. The importance of the acoustic velocity in the calculation of the fluctuating reaction rate had also been proposed previously by Beckstead and Brooks[40] and Rudinger.[41]

Comparison with Experimental Work

Using an r_{inf} value of 25 and an emissivity value of 0.25, the Rijke acoustic model was compared to the work of Barron[5] (see Fig. 11). The acoustic growth values predicted by the new Rijke model compare reasonably well with the experimental data at low concentration. The order of magnitude of the acoustic growth rate is correct, and there is an increase in acoustic growth for larger flow rates of aluminum particles. At higher aluminum concentrations, however, the model and experiment are more dissimilar. Reasons for such variations could stem from either the model or experimental data.

Certain aspects of this experimental data remain in question. A precise, constant flow in the particle feeder has been

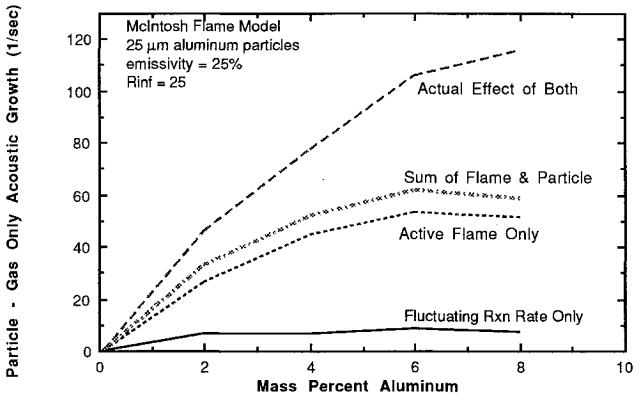

Fig. 10 Increase in acoustic growth due to addition of aluminum with and without fluctuating reaction rate and acoustically active flame. Note sharp increase with combined effects as compared to the algebraic sum of individual effects.

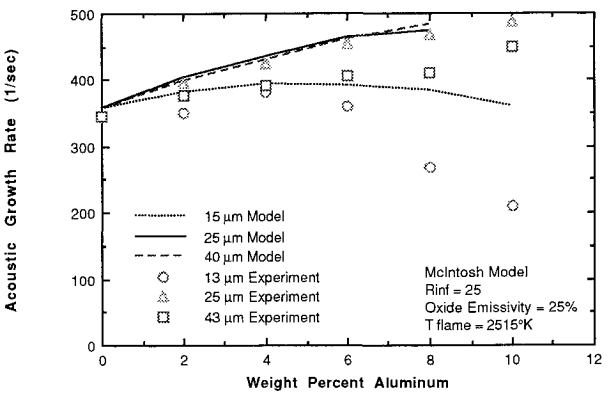

Fig. 11 Acoustic growth as a function of weight percent aluminum for the Rijke acoustic model and the experimental work of Barron (1991).

difficult to obtain, especially for small particle sizes. It has been suggested that the drop in acoustic growth for the 15-μm aluminum particles could be the result of fluctuations in the particle feed rate. At high aluminum mass fluxes, such errors are magnified, resulting in the larger data scatter at high concentrations. In addition, the particles used experimentally are not a single diameter, but rather a wide size distribution, resulting in varying burning rates and heat transfer characteristics. Efforts are currently underway to obtain improved experimental data and resolve the particle feeder and size distribution difficulties.

The model assumes that the particles burn as individuals, not affected by other particles surrounding them. At concentrations greater than 8% aluminum, group combustion is possibly occurring based on photographs taken of the experiment. Individual particles cannot be seen during aluminum combustion in the Rijke burner; only a bright ball of fire exists in the reaction zone. Under these conditions, the combustion mechanism could be different and the assumptions of the mean and oscillatory aluminum reaction models could break down. According to Chiu (taken from Kuo[15]), even 1% aluminum could result in group combustion for the size particles in question. However, Chiu assumes that the oxidizer must diffuse from the surroundings into the cloud for combustion to occur. In the case of the Rijke burner, the particles are premixed with the oxidizer, thus, the equations of Chiu would have to be rederived for this situation.

Conclusions

Law's aluminum combustion model has been expanded to include the effects of multiple oxidizers and their products, oxide accumulation on the surface of the burning aluminum particle, and convection. There are no adjustable parameters in the improved aluminum combustion model, and both transport and thermodynamic properties are calculated internally for varying temperature.

The aluminum combustion model has been compared to experimental data from burners, laser-ignited particles, and propellant under a variety of conditions. In spite of large data scatter, the aluminum combustion model compares more favorably to experimental data than a simple liquid droplet model. The discrepancy in the comparison between the model and experimental data is believed to be due both to difficulties in obtaining experimental data and shortcomings of the model due to the complexity of aluminum combustion. Calculations also indicated that simple empirical models, based on a summed mole fraction of oxidizer, could be erroneous in environments that contain several oxidizing species.

Three relatively recent models that have been compared here are either a direct derivative of, or are very similar to, Law's model,[12] and produce very similar results. However, there are significant differences. The Bhatia–Sirignano model seems to have the best agreement with the basic data. The Turns–Wong model is closer to agreement with the data if the surface inhibition due to the oxide cap is neglected. In the current model this is also true. Thus, the assumption of the oxide cap inhibiting the reacting surface area may not be a good assumption. Also, it is not clear why the Bhatia–Sirignano model overpredicts the dependency on O_2, while the other two models seem to predict this dependency correctly. Further studies are needed to clarify the physical characteristics that result in these apparent discrepancies.

The aluminum combustion model was incorporated into the Rijke program, and the mean and acoustic properties of the burner were studied separately. Efforts to characterize the location and amount of heat transfer between phases yielded the following:

1) Comparison with experimental work suggests an ignition temperature of ~1900 K for conditions found in the Rijke burner.

2) The size of the aluminum particle, the concentration of the aluminum and its oxidizer, and the emissivity of the metal oxide were all found to have a significant influence on the gas temperature profile.

The effects of aluminum combustion on the acoustics in the burner were determined by carrying out linear perturbation of the time-mean aluminum combustion model. Similar to the results of Raun, the increase in acoustic growth due to the addition of aluminum was much lower than corresponding experimental data. Using the more complex model of aluminum combustion did not appear sufficient to cause the proper increase in acoustic growth. The flame/acoustic interaction and the fluctuating reaction rate were studied to improve the fit of the experimental data.

Calculations have shown that a significant part of the acoustic growth with the addition of aluminum is due strictly to the change in the gas temperature profile. The change in temperature profile apparently causes the location of the velocity antinode to shift relative to the Rijke burner flame and thereby cause an increase in the flame response. The flame response can also couple with the fluctuating particle reaction rate resulting in a synergistic increase in acoustic growth over the individual effects.

To further improve the fluctuating aluminum combustion model, a time lag between the acoustic properties and the fluctuating heat release was added. This time lag is based on the length of time needed for an effect in the bulk to be transmitted to the aluminum diffusion flame through the boundary layer. For a boundary-layer thickness of approximately 25 particle diameters, the time lag shifted the effects of the acoustic velocity 90 deg out of phase. Such a boundary-layer thickness is very reasonable, and results in the heat release being in phase with the acoustic pressure, yielding a maximum in the acoustic driving.

The new Rijke acoustic model agreed within 10% of the acoustic growth rates observed by Barron for 25-μm aluminum particles. Discrepancies between experiment and model for the 13- and 43-μm aluminum particles were larger, but similar qualitative trends were seen.

References

[1]Braithwaite, P. C., "Measurements of Distributed Combustion in the Rijke Burner," M.S. Thesis, Brigham Young Univ., Provo, UT, Dec. 1984; see also Braithwaite, P. C., Beckstead, M. W., and Raun, R. L., "Measurements of Distributed Combustion," *21st JANNAF Combustion Meeting*, Vol. I, CPIA 412, 1984, pp. 177–186.

[2]Beckstead, M. W., Braithwaite, P. C., and Gordon, D. L., "Measurements of Distributed Combustion," *Smokeless Propellants*, AGARD-CP-391, 1985, p. 21-1.

[3]Finlinson, J. C., "Experimental Characterization of a Modified Rijke Burner," M.S. Thesis, Brigham Young Univ., Provo, UT, June 1988; see also Finlinson, J. C., Nelson, M. A., and Beckstead, M. W., "Characterization of a Modified Rijke Burner for Measurement of Distributed Combustion," *24th JANNAF Combustion Meeting*, Vol. I, CPIA 476, 1987, pp. 13–26.

[4]Raun, R. L., "A Numerical Model for the Rijke Burner," Ph.D. Dissertation, Brigham Young Univ., Provo, UT, Dec. 1985.

[5]Barron, J. T., "An Experimental Study on the Effects of Dispersed Particles on Acoustic Growth Rates in a Modified Rijke Burner," M.S. Thesis, Brigham Young Univ., Provo, UT, Aug. 1991.

[6]Raun, R. L., and Beckstead, M. W., "A Numerical Model for Temperature Gradient Effects on Rijke Burner Oscillations," *Combustion and Flame*, Vol. 94, Nos. 1/2, 1993, pp. 1–24.

[7]Raun, R. L., Beckstead, M. W., Finlinson, J. C., and Brooks, K. P., "A Review of Rijke Tubes, Rijke Burners and Related Devices," *Progress in Combustion Energy and Science*, Vol. 19, No. 4, 1993, pp. 313–364.

[8]Friedman, R., and Macek, A., "Ignition and Combustion of Aluminum Particles in Hot Ambient Gases," *Combustion and Flame*, Vol. 6, March 1962, pp. 9–19.

[9]Kuehl, D., "Ignition and Combustion of Aluminum and Beryllium," *AIAA Journal*, Vol. 3, No. 12, 1965, p. 2239–2247.

[10]Price, E. W., "Combustion of Metallized Propellants," *Fundamentals of Solid-Propellant Combustion*, Vol. 90, Progress in Astro-

nautics and Aeronautics, AIAA, New York, 1984, pp. 479–513; see also Price, E. W., Kraeutle, K. J., Prentice, J. L., Boggs, T. L., Crump, J. E., and Zurn, D. E., "Behavior of Aluminum in Solid Propellant Combustion," Naval Weapons Center, NWC TP 6120, China Lake, CA, March 1982.

[11]Razdobreev, A. A., Skorik, A. I., and Frolov, Yu. V., "Ignition and Combustion Mechanism in Aluminum Particles," *Combustion, Explosion, and Shock Waves*, Vol. 12, No. 2, 1976, pp. 203–207.

[12]Law, C. K., "A Simplified Theoretical Model for the Vapor-Phase Combustion of Metal Particles," *Combustion Science and Technology*, Vol. 7, 1973, pp. 197–212.

[13]Pokhil, P. F., Belyayev, A. F., Frolov, Yu. V., Logachev, V. S., and Korotkov, A. I., "Combustion of Powdered Metals in Active Media," FTD-MT-24-551-73, Oct. 1973.

[14]King, M. K., "Modeling of Single Particle Aluminum Combustion in CO_2-N_2 Atmospheres," *17th Symposium (International) on Combustion*, The Combustion Inst., Pittsburgh, PA, 1977, pp. 1317–1328.

[15]Kuo, K. K., *Principles of Combustion*, Wiley, New York, 1986.

[16]Micheli, P. L., and Schmidt, W. G., "Behavior of Aluminum in Solid Rocket Motors," Aerojet Solid Propulsion Co., AFRPL-TR-76-58, Sacramento, CA, Jan. 1977.

[17]Brzustowski, T. A., and Glassman, I., "Spectroscopic Investigation of Metal Combustion," Vol. 15, *Heterogeneous Combustion*, Progress in Astronautics and Aeronautics, AIAA, New York, 1964a, pp. 41–73; see also "Vapor-Phase Diffusion Flames in the Combustion of Magnesium and Aluminum I. Analytical Developments," pp. 75–115.

[18]Glassman, I., *Combustion*, Academic, New York, 1977.

[19]Law, C. K., and Williams, F. A., "On a Class of Models for Droplet Combustion," AIAA Paper 74-147, Jan. 1974.

[20]Gremyachkin, V. M., Istratov, A. G., and Leipunskii, O. I., "Effect of Immersion in a Flow on Metal-Drop Combustion," *Combustion, Explosion, and Shock Waves*, Vol. 15, No. 1, 1979, pp. 26–29.

[21]Gremyachkin, V. M., Istratov, A. G., and Leipunskii, O. I., "Model for the Combustion of Metal Droplets," *Combustion, Explosion, and Shock Waves*, Vol. 11, No. 3, 1975, pp. 313–318.

[22]Kudryavtsev, V. M., Sukhov, A. V., Voronetskii, A. V., and Shpara, A. P., "High Pressure Combustion of Metals (Three-Zone Model)," *Combustion, Explosion, and Shock Waves*, Vol. 15, No. 6, 1979, pp. 731–737.

[23]Turns, S. R., Wong, S. C., and Ryba, E., "Combustion of Aluminum-Based Slurry Agglomerates," *Combustion Science and Technology*, Vol. 54, Nos. 1–6, 1987, pp. 299–318.

[24]Bhatia, R., and Sirignano, W. A., "Metal Particle Combustion with Oxide Condensation," *Combustion Science and Technology* (to be published).

[25]Brooks, K. P., "Characterization of the Flame and Aluminum Particles in a Rijke Burner," M.S. Thesis, Brigham Young Univ., Provo, UT, Dec. 1992; see also Brooks, K. P., and Beckstead, M. W., "Evaluation of a Flame Model with a Rijke Burner," *28th JANNAF Combustion Meeting*, Vol. II, CPIA 573, 1991, pp. 509–517.

[26]Chung, S. H., and Law, C. K., "Importance of Dissociation Equilibrium and Variable Transport Properties on Estimation of Flame Temperature and Droplet Burning Rate," *Combustion and Flame*, Vol. 55, 1984, pp. 225–235.

[27]Frank-Kamenetski, D. A., *Diffusion and Heat Transfer in Chemical Kinetics*, Plenum, New York, 1969.

[28]Hunter, H. W., "Aluminum Particle Combustion Progress Report," Naval Ordnance Test Station, NOTS TP 3916, China Lake, CA, April 1964–June 1965.

[29]Prentice, J. L., "Aluminum Droplet Combustion: Rates and Mechanisms in Wet and Dry Oxidizers," Naval Weapons Center, NWC TP 5569, China Lake, CA, April 1974.

[30]Davis, A., "Solid Propellants: The Combustion of Particles of Metal Ingredients," *Combustion and Flame*, Vol. 7, Dec. 1963, pp. 359–367.

[31]Wilson, R. P., Jr., and Williams, F. A., "Experimental Study of the Combustion of Single Aluminum Particles in O_2/Ar," *Thirteenth Symposium (International) on Combustion*, The Combustion Inst., Pittsburgh, PA, 1971, pp. 833–845.

[32]Friedman, R., and Macek, A., "Combustion Studies of Single Aluminum Particles," *Ninth Symposium (International) on Combustion*, Academic, New York, 1963, pp. 703–712.

[33]Macek, A., "Fundamentals of Combustion of Single Aluminum and Beryllium Particles," *Eleventh Symposium (International) on Combustion*, The Combustion Inst., Pittsburgh, PA, 1967, pp. 203–214.

[34]Hartman, K. O., "Ignition and Combustion of Aluminum Particles in Propellant Flame Gases," *8th JANNAF Combustion Meeting*, Vol. 1, CPIA 220, 1971, pp. 1–24.

[35]Wong, S.-C., and Turns, S. R., "Ignition of Aluminum Slurry Droplets," *Combustion Science and Technology*, Vol. 52, Nos. 4–6, 1987, pp. 221–242.

[36]Rayleigh, J. W. S., "The Explanation of Certain Acoustical Phenomena," *Nature*, Vol. 18, 1878, pp. 319–321.

[37]Bailey, J. J., "A Type of Flame-Excited Oscillation in a Tube," *Journal of Applied Mechanics*, Vol. 24, No. 3, 1957, pp. 333–339.

[38]Glassman, I., Papas, P., and Brezinsky, K., "A New Definition and Theory of Metal Pyrophoricity," *Combustion Science and Technology*, Vol. 83, Nos. 1–3, 1992, pp. 161–165.

[39]Musarra, S. P., Fletcher, T. H., Niksa, S., and Dwyer, H. A., "Heat and Mass Transfer in the Vicinity of a Devolatilizing Coal Particle," *Combustion Science and Technology*, Vol. 45, 1986, pp. 289–307.

[40]Beckstead, M. W., and Brooks, K. P., "A Model for Distributed Combustion in Solid Propellants," *27th JANNAF Combustion Meeting*, Vol. II, 1990, pp. 237–258.

[41]Rudinger, G., "Effect of Velocity Slip on the Burning Rate of Fuel Particles," *Journal of Fluids Engineering*, Sept. 1975, pp. 321–326.